

Enamine/Dienamine and Brønsted Acid Catalysis: Elusive Intermediates, Reaction Mechanisms, and Stereoinduction Modes Based on in Situ NMR Spectroscopy and Computational Studies

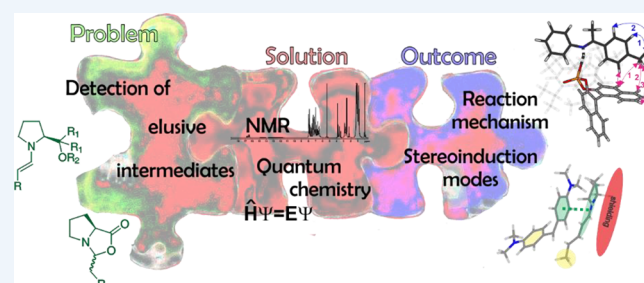
Polysena Renzi,¹ Johnny Hioe, and Ruth M. Gschwind*¹

Institut für Organische Chemie, Universität Regensburg, D-95053 Regensburg, Germany

CONSPECTUS: Over the years, the field of enantioselective organocatalysis has seen unparalleled growth in the development of novel synthetic applications with respect to mechanistic investigations. Reaction optimization appeared to be rather empirical than rational. This offset between synthetic development and mechanistic understanding was and is generally due to the difficulties in detecting reactive intermediates and the inability to experimentally evaluate transition states. Thus, the first key point for mechanistic studies is detecting elusive intermediates and characterizing them in terms of their structure, stability, formation pathways, and kinetic properties. The second key point is evaluating the importance of these intermediates and their properties in the transition state.

In the past 7 years, our group has addressed the problems with detecting elusive intermediates in organocatalysis by means of NMR spectroscopy and eventually theoretical calculations. Two main activation modes were extensively investigated: secondary amine catalysis and, very recently, Brønsted acid catalysis. Using these examples, we discuss potential methods to stabilize intermediates via intermolecular interactions; to elucidate their structures, formation pathways and kinetics; to change the kinetics of the reactions; and to address their relevance in transition states. The elusive enamine in proline-catalyzed aldol reactions is used as an example of the stabilization of intermediates via inter- and intramolecular interactions; the determination of kinetics on its formation pathway is discussed. Classical structural characterization of intermediates is described using prolinol and prolinol ether enamines and dienamines. The *Z/E* dilemma for the second double bond of the dienamines shows how the kinetics of a reaction can be changed to allow for the detection of reaction intermediates. We recently started to investigate substrate–catalyst complexes in the field of Brønsted acid catalysis. These studies on imine/chiral phosphoric acid complexes show that an appropriate combination of highly developed NMR and theoretical methods can provide detailed insights into the complicated structures, exchange kinetics, and H-bonding properties of chiral ion pairs. Furthermore, the merging of these structural investigations and photoisomerization even allowed the active transition state combinations to be determined for the first time on the basis of experimental data only, which is the gold standard in mechanistic investigations and was previously thought to be exclusively the domain of theoretical calculations.

Thus, this Account summarizes our recent mechanistic work in the field of organocatalysis and explains the potential methods for addressing the central questions in mechanistic studies: stabilization of intermediates, elucidation of structures and formation pathways, and addressing transition state combinations experimentally.



■ INTRODUCTION

In its infancy, the field of organocatalysis saw rapid growth in terms of novel synthetic applications with a general lack of rational mechanistic understanding.¹ Reaction optimization appeared to be empirical rather than rational because the understanding of reaction mechanisms, the characterization of competing unwanted reactions, and ultimately the rational design and optimization of reactions require knowledge of intermediate structures, stability, and formation pathways.

The ability of NMR spectroscopy to provide information not only about reactant structures but also about their aggregation states and intermolecular interactions in solution makes NMR methods extremely valuable for clarification of reaction mechanisms. Furthermore, in ideal situations, the profound

structural information gained by these techniques may serve as an important input for theoretical calculations and be used to validate or even further develop theoretical methods. Moreover, real reaction conditions can be directly studied in situ since the concentration requirements for NMR experiments are often close to those of synthetic applications, especially in organocatalytic reactions. Despite these advantages, there are also well-known and often critical limitations. For organocatalytic studies, low NMR sensitivity and poor time resolution impede the detection of interactions and short-lived/low-populated intermediates. Furthermore, in complex reaction mixtures,

Received: June 27, 2017

Published: November 27, 2017

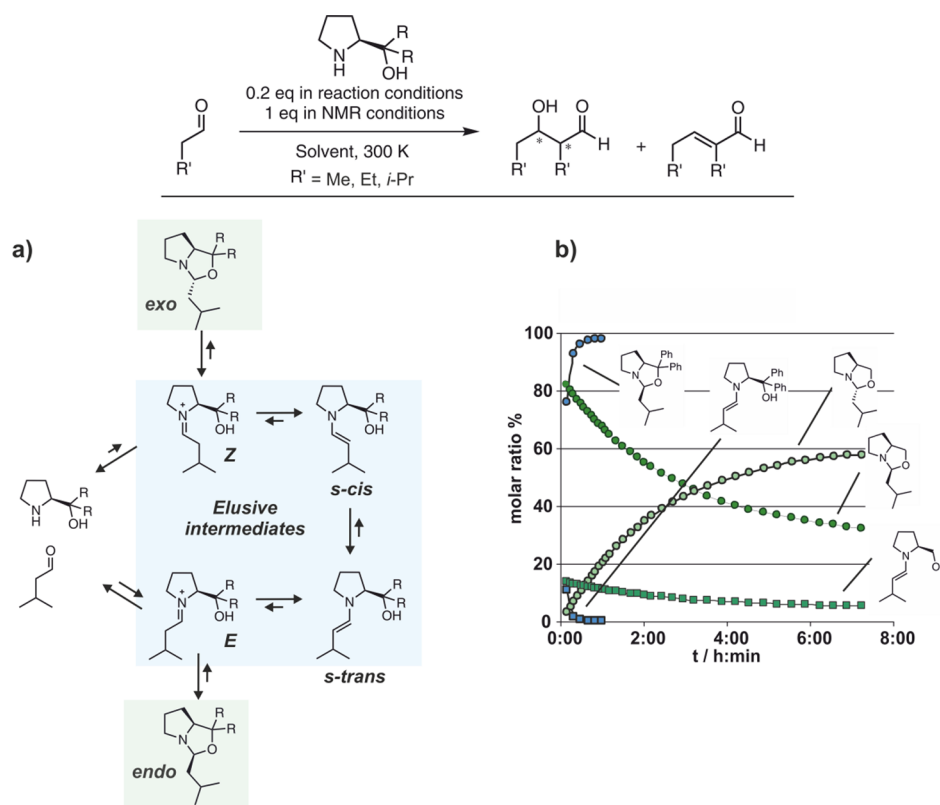


Figure 1. L-Proline-catalyzed self-aldolization of aldehydes. (a) Proposed equilibria between starting materials, iminium ions, enamines, and oxazolidines.⁷ (b) Evolution of intermediates derived from isovaleraldehyde and prolinol-type organocatalysts in DMSO- d_6 monitored by 1D ^1H NMR spectroscopy. Adapted from ref 7. Copyright 2011 American Chemical Society.

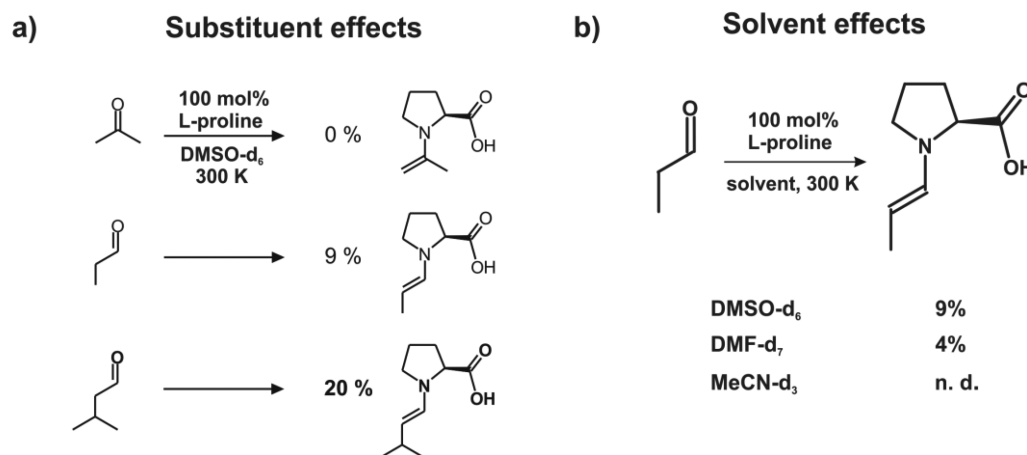


Figure 2. (a) Substituent and (b) solvent effects on enamine detection. The percentages shown refer to the maximum amounts of enamine intermediate detected in the reaction (total amount of intermediates equals 100%). Adapted with permission from ref 4. Copyright 2010 John Wiley and Sons.

spectral overlap of similar species and the connection between intermediates and transition states (TSs) are generally difficult to resolve without theoretical calculations.

This Account will discuss the problems mentioned above and our approach to solving them. First, in enamine catalysis, the low stability and complicated equilibria between intermediates impeded enamine detection and structural investigation. In dienamine catalysis, the reaction topography was not consistent with the requirements for monitoring. In the prototypical chiral phosphoric acid (CPA)-catalyzed transfer hydrogenation of imines, the structural investigation of the proto-binary complex

was hindered by severe spectral complexity. In the last section of this Account, we highlight our recent progress in decoding experimentally active TS combinations by merging NMR spectroscopy with photoisomerization. The arsenal of solutions presented in this Account ranges from technical aspects in terms of NMR spectroscopy, understanding of complex equilibria between intermediates, and adjustment of reaction kinetic profiles to the application of external stimuli to decrypt undetectable TSs.

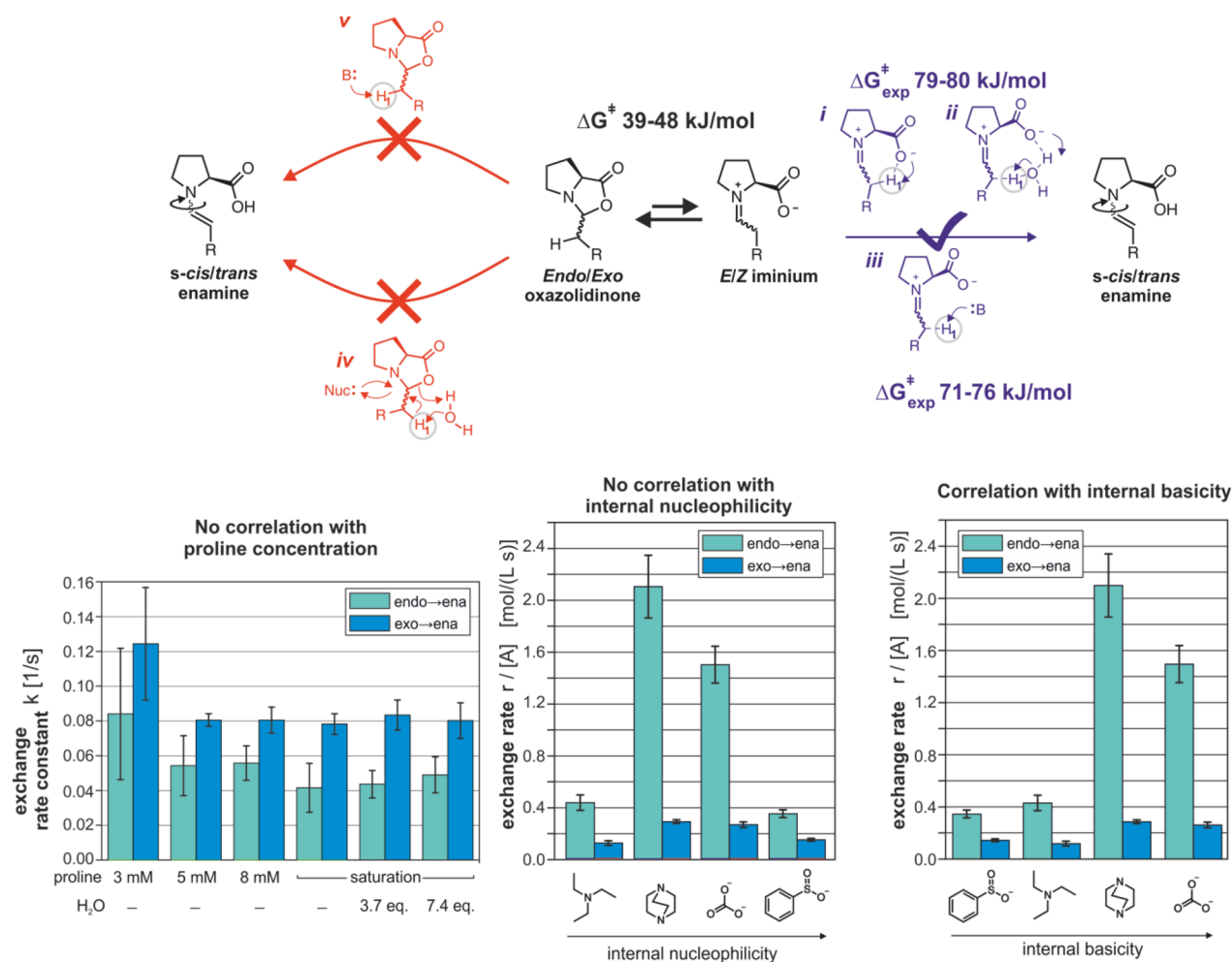


Figure 3. Summary of the proposed enamine formation pathways. Adapted from ref 8. Copyright 2015 American Chemical Society.

■ ENAMINE CATALYSIS: DETECTION OF INTERMEDIATES AND MECHANISTIC INSIGHTS

Enamine catalysis is one of the most prominent methods for the enantioselective α -functionalization of carbonyl compounds.² The first synthetic application, known as the Hajos–Parrish–Eder–Sauer–Wiechert reaction, dates back to 1974.³ Despite many synthetic advances and developments in the past 50 years, detection of the key enamine intermediate remained one of the biggest challenges in spectroscopy. The first in situ detection and characterization of this important reactive intermediate was achieved in our working group in 2010 using NMR spectroscopy.⁴ Parallel to our work, List and co-workers reported the crystal structures of stabilized fluoro-substituted enamines.⁵ The formation of the experimentally detectable *endo/exo*-oxazolidinones/oxazolidinones from prolinol/proline catalysts was in fact postulated to be a “parasitic equilibrium” or even a “dead end”.⁶ This escape mechanism was thought to be responsible for the short lifetime of the enamine in the catalytic cycle. Therefore, the key to success was to understand the stabilization modes of enamines versus oxazolidinones/oxazolidinones (Figure 1a).^{4,7}

As shown by our extensive studies, the detection of enamines is very delicate and is dependent on the H-bond acceptor ability of the solvent and the substitution pattern of the aldehyde (Figure 2a,b).⁷ First, substituent effects within the five-membered oxazolidinone/oxazolidinone ring were analyzed.

Digeminal substitution using ketones (Figure 2a) and/or aromatic groups on the catalyst shielding moiety (Figure 1b, blue) promotes ring closure via the Thorpe–Ingold effect. Hence, enamines derived from diphenylprolinol are virtually removed from the catalytic cycle, whereas those from prolinol can be detected in solution (Figure 1b, green). The enamine intermediate can be accumulated by slowing the aldolization process via β -substitution of the aldehyde (Figure 2a) and employing H-bond-accepting solvents, which stabilize the enamine intermediate (Figure 2b).⁴

By knowledge of these effects and the use of equimolar mixtures of aldehyde and secondary amine in DMSO-*d*₆, the amount of the previously elusive enamine could be increased to as much as 20% of the detectable intermediates, allowing for full structural characterization. The NMR spectroscopic assignments of this complex mixture of starting material, intermediates, and products were accomplished by recording short-period HSQC/COSY spectra at various times during the reaction. Furthermore, repetition of the measurements on freshly prepared samples in combination with the high sensitivity of a cryoprobe drastically enhanced the signal intensity and allowed extensive assignment of intermediates.^{4,7,8,16}

Having established a correlation between enamine concentration and reactivity,⁷ we focused again on proline enamine formation pathways.⁸ While it was generally accepted that the enamine is formed via an iminium intermediate,^{9–11} no direct

experimental evidence existed until recently. 2D exchange spectroscopy (EXSY) experiments⁴ showing exchange peaks between the oxazolidinones and enamines suggested that base-assisted enamine formation occurs directly from the oxazolidinone, as previously proposed by Seebach (E2 elimination).¹² However, reliable kinetic information from 2D spectra could not be obtained since the mixing times (τ_{mix}) necessary for acceptable signal/noise ratios were far greater than the initial linear buildup region. Fine-tuning of the synthetic and spectroscopic techniques (dry DMSO, optimal aldehyde substitution pattern, and selective 1D EXSY spectra) was necessary to obtain reliable kinetic information and allow mechanistic questions about a particular step in the reaction mechanism to be answered. Thus, the rate of enamine formation in DMSO was quantitatively determined by selective 1D ¹H EXSY and compared with that obtained by high-level theoretical calculations at the coupled cluster singles, doubles, and perturbative triples/complete basis set (CCSD(T)/CBS) level for interpretation and validation.⁸

Different iminium pathways for enamine formation were proposed (Figure 3) and rationalized by theoretical calculations, mainly using density functional theory (DFT).^{10,11} In most cases, DFT is still the first choice in computational chemistry. To obtain quantitative reaction energies and rates, higher theoretical levels, such as perturbation theory or coupled cluster theory, with very large basis sets are usually necessary. Currently, the efficient implementation of domain-based local pair natural orbital (DLPNO) in coupled cluster theory allows the calculation of moderately large molecules (~100 atoms).¹³ Nevertheless, even at very high levels of theory such as CCSD(T), significant deviations between theory and experiment may be observed. Often this failure can be attributed to the incomplete description of solvent effects. Several solutions are available, ranging from the implicit solvation model and cluster continuum model to explicit solvation. While implicit solvation is computationally easy, it is not able to mimic the explicit interactions between solute and solvent (e.g., H-bonding), which can be taken into account by the inclusion of explicit solvent molecules (cluster continuum model). The impact of such explicit solvent molecules in the calculation of the stability of enamines was shown by Blackmond and Houk^{14a} as well as by Sunoj^{14b} and Smith.^{14c} In the absence of solvent molecules, the enamine is thermodynamically very unstable. Hence, an explicit solvent molecule is compulsory in this investigation.

Our calculations showed that the ring-opening step of the oxazolidinone to form the iminium is several orders of magnitude faster than the proton abstraction leading to the enamine. This means that the latter is the rate-determining step (RDS) for enamine formation and must be compared to the experimental data. Our EXSY measurements and theoretical calculations revealed that in the absence of basic additives, the formation of the enamine is water-assisted and faster from *exo*-oxazolidinone (Figure 3, paths *i* and *ii*: $\Delta G_{\text{exp}}^{\ddagger}(\text{exo} \rightarrow \text{ena}) = 79$ kJ/mol and $\Delta G_{\text{exp}}^{\ddagger}(\text{endo} \rightarrow \text{ena}) = 80$ kJ/mol). The enamine formation, especially from the *endo*-oxazolidinone, is accelerated significantly by bases, and the acceleration is correlated with the strength of the base (Figure 3, path *iii*: $\Delta G_{\text{exp}}^{\ddagger}(\text{endo} \rightarrow \text{ena}) = 71\text{--}76$ kJ/mol). This result confirmed the pathways proposed by List and Houk (Figure 3, paths *i*–*iii*) based on the generation of enamines via iminium ions.¹⁰ Alternative enamine pathways via an oxazolidinone (Figure 3, paths *iv* and *v*), either nucleophile- or base-assisted, were also proposed. However, the

experimental enamine formation rate is independent of proline concentration or additive nucleophilicity. This result excludes participation of the nucleophile or the proline derivative in the oxazolidinone ring opening as depicted in pathways *iv* and *v* under our experimental conditions. Furthermore, ongoing studies using enhanced NMR methods allowed for the direct detection of the iminium intermediate.

However, parallel to our study,⁸ Veticat and co-workers performed kinetic isotope effect (KIE) studies and a computational study of similar reactions in acetonitrile and showed that E2 elimination pathway *v* is indeed possible.¹⁵ However, for the KIE experiments to be applicable, the enamine formation itself must be the RDS, while for NMR studies to be effective, the RDS must occur after the formation of the enamine intermediate. Thus, this reaction is an excellent example of the existence of multiple mechanistic pathways in catalytic reactions in the case of deviating experimental conditions.

NMR CONFORMATIONAL ANALYSIS OF PROLINOL/PROLINOL ETHER ENAMINES/DIENAMINES

The full conformational analysis of prolinol/prolinol ether-derived enamines was accomplished by exploiting the expertise gained during our investigation of proline-derived enamines and applying ¹H,¹H NOESY and coupling constant analysis.¹⁶ First, a characteristic and well-separated proton signal is required (e.g., H₁ for enamines; Figure 4). The conformation

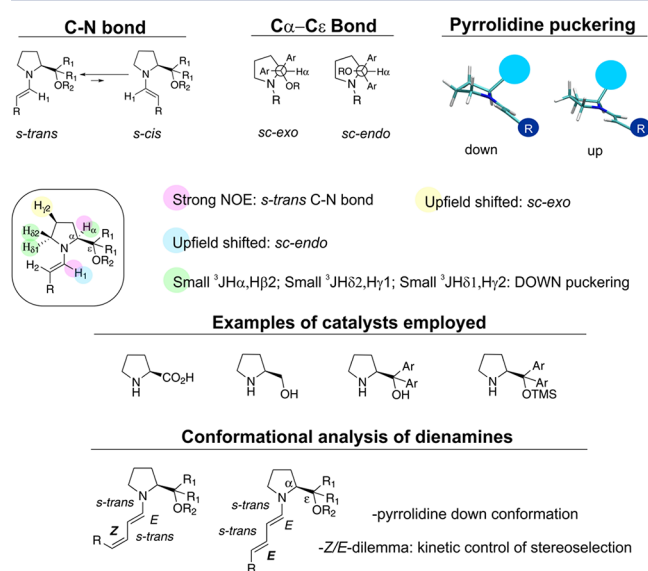


Figure 4. Conformational analysis of diaryl(ether)-prolinol di/enamines. Adapted with permission from refs 16 and 18. Copyright 2011 Royal Society of Chemistry and 2016 American Chemical Society, respectively.

is then determined by analyzing the relative intensities of the NOEs and the homo/heteronuclear coupling constants. The preference for the *s-trans* conformation was proven by a strong NOE between H₁ and H_α and confirmed by the cross-peak intensity between H₁ and C_α in the HMBC experiment. The *E* configuration of the double bond was confirmed by coupling constant analysis (Figure 4).

The puckering of the pyrrolidine ring is associated with enamine reactivity, and it is therefore an important parameter to determine.¹⁷ Generally, two pucker conformations were

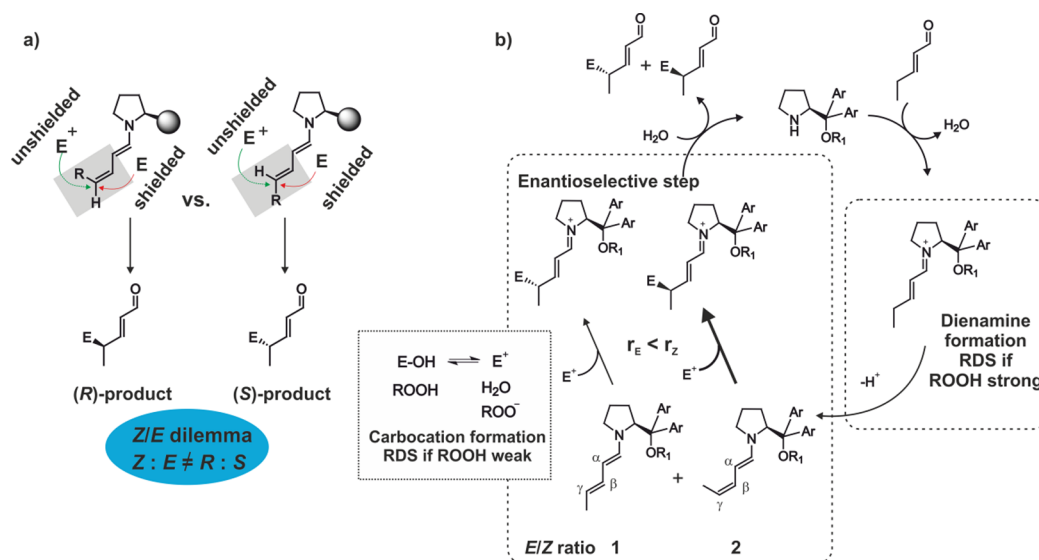


Figure 5. Dienamine catalysis: (a) the E/Z dilemma; (b) γ -functionalization of pentenal. Different acids were used to detect the dienamines and shift the RDS. Adapted from ref 18. Copyright 2016 American Chemical Society.

considered: the concave/up conformation and the convex/down conformation (Figure 4). The conformational preference of the ring can be measured via 3J scalar couplings between H_{α} and $H_{\beta 2}$ and between $H_{\delta 2}$ and $H_{\gamma 1}$. In the down conformation, small values for $^3J(H_{\alpha}, H_{\beta 2})$ and $^3J(H_{\delta 2}, H_{\gamma 1})$ are observed, while small values for $^3J(H_{\delta 1}, H_{\gamma 2})$ are indicative of the up conformation. Interestingly, the catalyst alone does not show any conformational preference; instead, a dynamic equilibrium is established between the two forms ($^3J(H_{\alpha}, H_{\beta 1/2}) > 7$ Hz). In contrast, enamine formation forces the pyrrolidine system to adopt the down conformation with all catalysts investigated to date. The experimental values for diaryl(ether)-prolinol enamines ($^3J(H_{\alpha}, H_{\beta 2}) = 1.5$ – 2.5 Hz) suggest a purely down pyrrolidine ring conformation, which is a vital steric requirement for electrophilic attack. In addition to NOESY analysis, a conformational screening method was developed to determine the C_{α} – C_{ϵ} bond conformation (*sc-endo/-exo*), which is directly reflected in the H_1 and $H_{\gamma 2}$ chemical shifts. Prolinol enamines were found to prefer the *sc-endo* conformation, whereas prolinol-ether enamines adopt the *sc-exo* conformation. Comparing the conformational preference with the stereoinduction mode of the prolinol enamines shows that the OH substituent may form H-bonds with the incoming electrophile, thus facilitating the upper-face selectivity, while the aryl substituent may serve as an effective shielding group. The conformational analysis of the dienamines revealed the same configurational preferences as those of enamine catalysis (Figure 4).¹⁸

This enamine study showed that understanding of the intra- and intermolecular stabilization modes of intermediates can facilitate the detection of elusive intermediates, the determination of structural preferences, and the acquisition of detailed insights into their formation pathways starting from other intermediates.

DIENAMINE CATALYSIS: MECHANISTIC INSIGHTS

The next step was to solve the “ E/Z dilemma”¹⁹ for the second double bond in dienamine catalysis:¹⁸ the Z/E ratios of the second double bond did not correlate with the experimental ee values if a classical shielding model was assumed (Figure 5a).

Furthermore, the preferred formation and the downstream reaction of the Z isomers was rationalized.

We chose the γ -alkylation of α,β -unsaturated aldehydes with Michler’s hydrol as a model system (Figure 5b).¹⁸ In accordance with previous studies,²⁰ an E/Z -dienamine ratio of $\sim 1/2$ was detected for 2-pentenal. If E/Z -dienamines react at the same rate, the ee should be 33%. However, this does not correlate with the experimental ee values (28–92% ee depending on the catalyst). Thus, either a different E/Z ratio is formed in the presence of the electrophile or the activation barriers vary significantly in the downstream reactions of the E - and Z -dienamines.

As expected, the theoretical calculations predicted the E -dienamine to be thermodynamically more stable. However, TS calculations corroborated the kinetic preference for the formation of the Z -dienamine, most likely due to steric interactions in the TS. NMR experiments confirmed a very slow $Z \rightarrow E$ isomerization and the 1/2 E/Z ratio, which correlate to the situation in the formation step. Therefore, the dienamine downstream reaction was studied. Unfortunately, the dienamine formation is followed by a fast electrophilic addition. As a result, dienamine intermediates cannot be detected under typical reaction conditions. To slow the electrophilic attack, it was necessary to reduce the amount of active electrophile present, not in terms of absolute starting concentration but in maintaining a steady-state concentration during the whole reaction. For Michler’s hydrol, this is possible by employing weak acids that release small amounts of the electrophilic carbocation. As a result, electrophile formation became the RDS, allowing detection of the dienamine by NMR spectroscopy (Figure 6a). Calculations confirmed that the TS of the attack on the Z -dienamine (TS- Z) is more stable than that of the E -form (TS- E). The structural and non-covalent interaction (NCI) analyses²¹ revealed two major interactions that favor TS- Z (Figure 6b) and are responsible for the variation in the ee values obtained with different catalysts. In summary, the delicate interplay of the substrate, catalyst, and electrophile results in highly effective remote stereocontrol in dienamine catalysis.

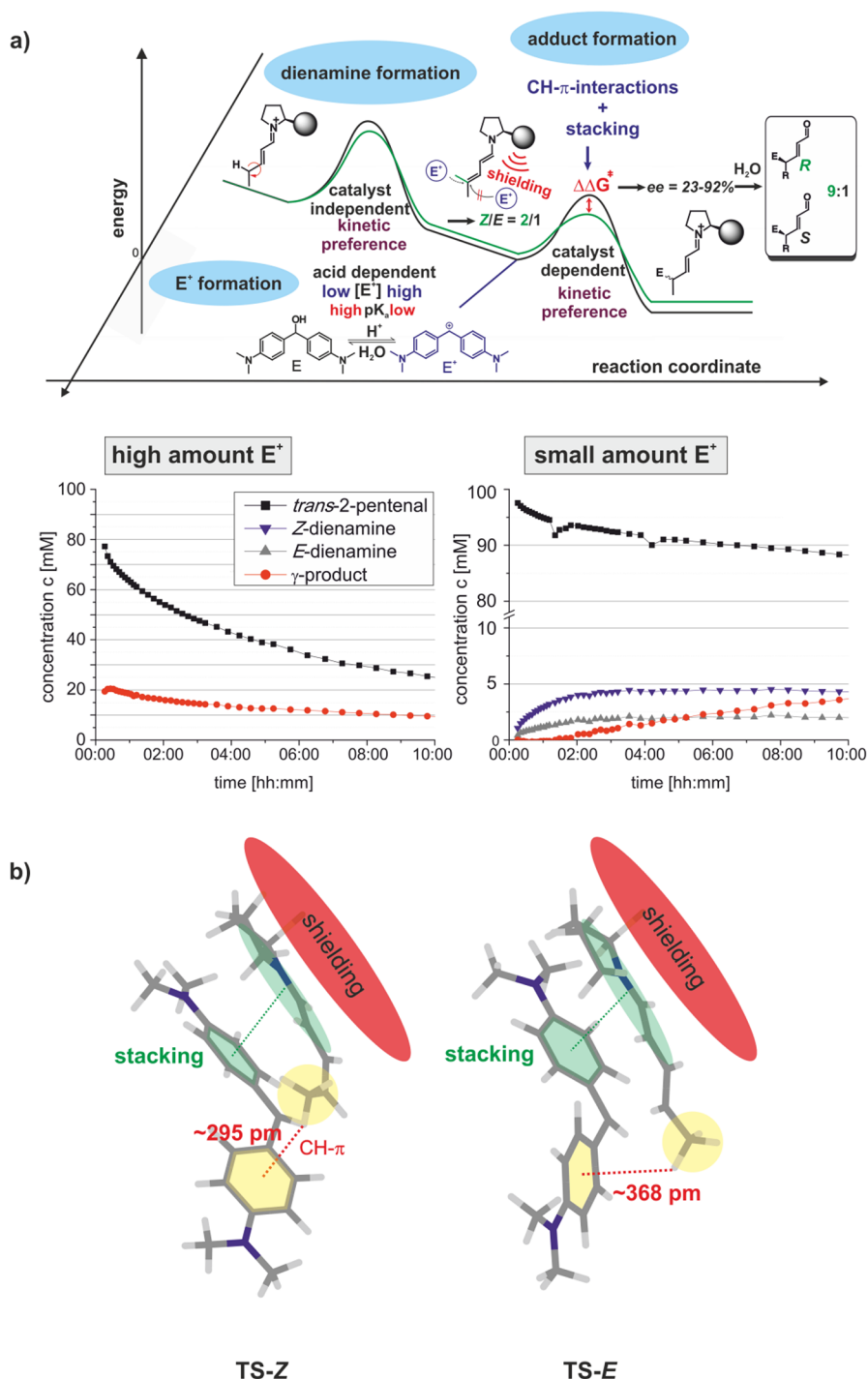
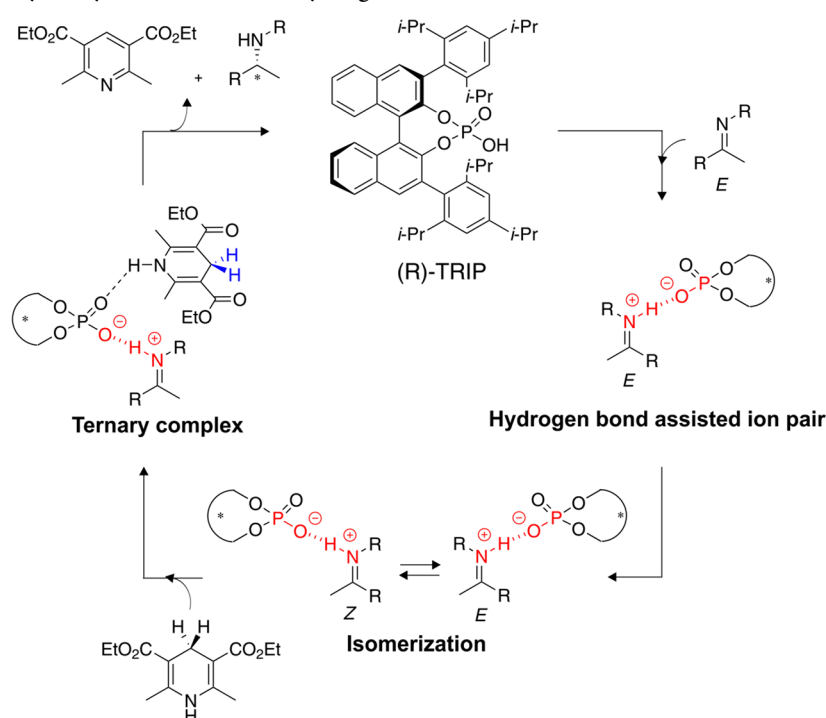


Figure 6. (a) Kinetic preference for Z-dienamine formation and consumption and (b) dispersive interactions favoring TS-Z. Adapted from ref 18. Copyright 2016 American Chemical Society.

■ ASYMMETRIC BRØNSTED ACID CATALYSIS

The success of chiral Brønsted acids in organocatalysis is linked to their broad applicability, high substrate tolerance, high yields, and excellent stereoselectivities.²² However, structural elucidation of intermediates or prereacting complexes stabilized by NCIs in solution appeared to be very difficult. For example, the purely electrostatic interactions driving asymmetric counteranion-directed catalysis²³ may simultaneously produce numerous structures. In contrast, the H-bond formation in chiral Brønsted acid catalysis has several advantages: (i) the strong charge-assisted H-bonds reduce the number of possible

complex structures; (ii) the extreme low-field H shift in strong H-bonds provides resolved signals that can be used as a starting point for structural investigation; and (iii) the H-bridges that consist of labeled or NMR-active nuclei allow the strategies developed for protein and small-molecule NMR spectroscopy to be used.^{24,25} Thus, considering our experience in PO–HN H-bridges,²⁶ we selected the asymmetric transfer hydrogenation of imines in the presence of CPAs as our model reaction.²⁷ CPAs contain ³¹P as a 100% NMR-active nucleus, and the target imine substrate can easily be ¹⁵N-labeled.

Scheme 1. Proposed Catalytic Cycle for Ketimine Hydrogenation^{27b,28}a) Toluene- d_8

Hydrogen bond region

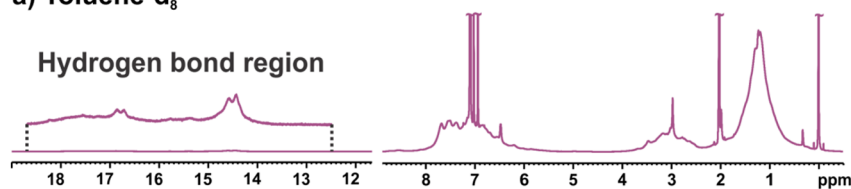
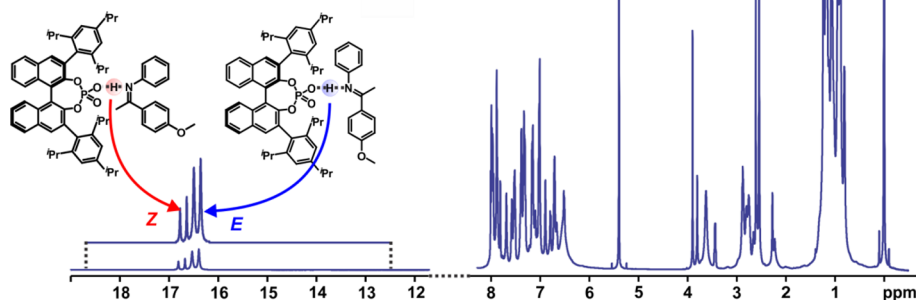
b) CD_2Cl_2 

Figure 7. Improvement of chemical shift resolution in the 1H NMR spectrum of an imine/catalyst complex in going from (a) toluene- d_8 to (b) CD_2Cl_2 at 180 K. Adapted from ref 34. Copyright 2016 American Chemical Society.

According to the catalytic cycle proposed by Rueping in 2005,^{27b} this transformation starts with the formation of a H-bond-assisted ion pair (binary complex) between the CPA and the imine. Subsequently, a fast *E/Z*-imine isomerization in the iminium ion binary complex was assumed, followed by the formation of a ternary complex with the Hantzsch ester (Scheme 1).

Until recently, only one example of NMR characterization of a ternary complex in solution existed;²⁹ most of the structural information had been provided by DFT calculations,²⁸ and X-ray structures were rare.³⁰ With this background, our aim was

to experimentally address the key points of the proposed mechanism and answer the following questions:

1. What is the H-bond situation in the imine/catalyst binary complex?
2. What is the structure of the binary complex?
3. Which TSs are involved in the reaction? Is it possible to access them experimentally?

The main problem encountered in the NMR study of reactions mediated by CPAs is the complicated overlap of signals in the aromatic region due to the aromatic structures of

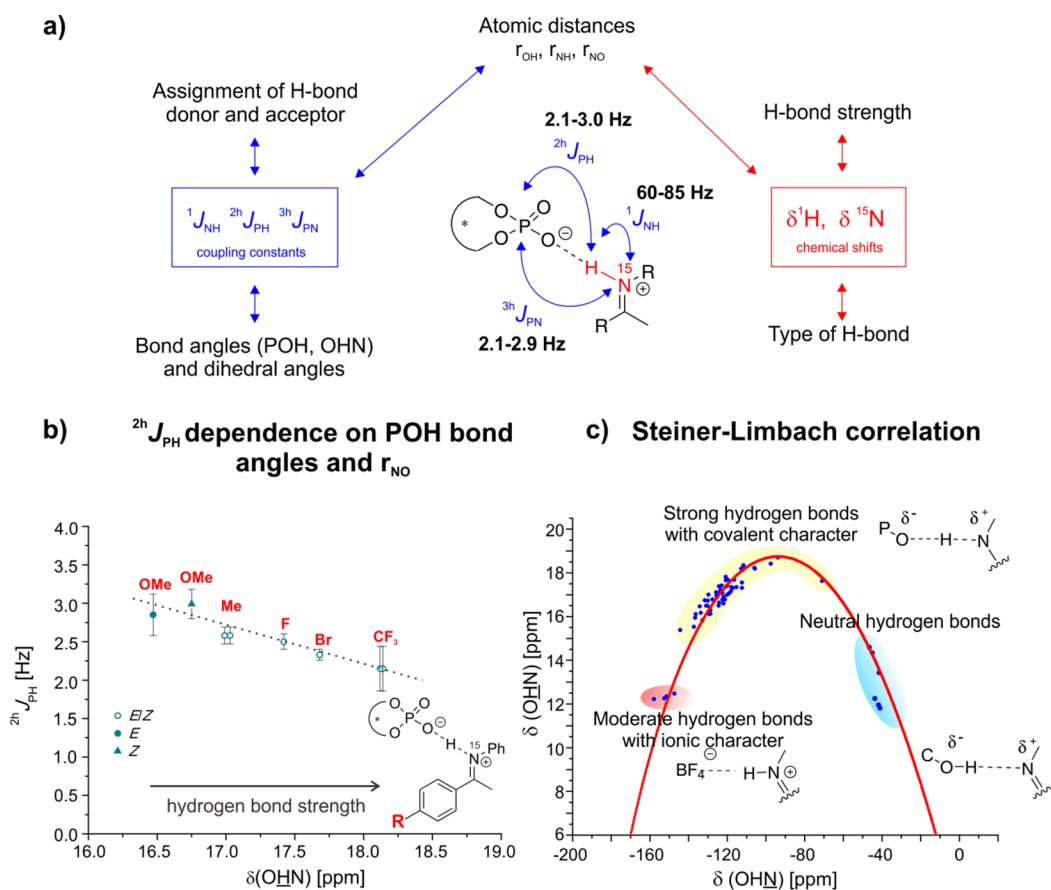


Figure 8. (a) Combination of strategies used to characterize H-bonds via (b) trans H-bond scalar couplings analysis and (c) a combination of chemical shift information. Adapted from ref 32. Copyright 2016 American Chemical Society.

both the catalyst and the imine. For this reason, our first study focused on investigating the H-bonding in the complex.³¹ To simplify the spectra, the achiral catalyst diphenyl phosphate was used in combination with ¹⁵N-labeled aldimines and ketimines. In these initial measurements, ¹H,¹⁵N magnetization transfers and coupling constants revealed the existence of iminium species. However, the low temperatures (240–180 K) necessary to resolve the sets of signals and allow the detection of H-bond signals revealed the formation of complicated mixtures of H-bonded species, which indicated broad conformational space and multiple aggregation states for the achiral catalyst. Thus, for the detailed analysis, we decided to employ a more sterically hindered CPA (TRIP).³² The use of this catalyst allowed the complete characterization of the properties and geometries of the imine/(R)-TRIP binary complexes and started with the well-resolved proton chemical shift region of the H-bonds (no overlap with other signals above 10 ppm).

The first challenge was the selection of the right conditions for our NMR experiments. As shown in Figure 7a, toluene-*d*₈ was not an appropriate solvent due to the extremely broad signals. Superior line widths and signal dispersion were obtained in CD₂Cl₂/freon mixtures (Figure 7b). Furthermore, equimolar amounts of ¹⁵N-labeled imine and (R)-TRIP were employed together with dry catalyst and anhydrous solvents to reduce imine hydrolysis.

The H-bond investigation started with an analysis of the chemical shifts in the region between 10 and 18 ppm and the ¹J_{NH} coupling constants. Two characteristic doublets were

obtained for the ¹⁵NH involved in the H-bond of each catalyst/imine combination (Figure 7b). Standard 2D ¹H,¹⁵N NOESY experiments at 180 K were performed to distinguish between the *E*- and *Z*-imines inside the complex using the separated signals of the NH in the H-bond and in the methyl group. By combining the magnetization transfers through H-bond scalar couplings used by Grezciek²⁴ in biomacromolecules with the H-bond analysis of small-molecule systems mainly developed by Limbach³³ (Figure 8a), we could completely characterize the H-bonds in the binary complex. Our general idea was to determine the H-bond strength, the type of H-bond, and the atomic distances (r_{OH} , r_{NH} , r_{NO}) from the ¹H and ¹⁵N chemical shifts by applying the Steiner–Limbach correlation (Figure 8c). Then the experimental coupling constants ($^{mh}J_{XY}$) between the nuclei connected through the H-bridge were used in combination with the distances derived from the Steiner–Limbach correlation to define the H-bond geometry.

According to the Steiner–Limbach correlation, the proton position within the H-bond can be modulated by varying the acidity and basicity of the donor and acceptor in a stepwise fashion.^{32,33} The parabolic dependence of the proton chemical shifts $\delta(OHN)$ in combination with the linear dependence of the nitrogen chemical shifts $\delta(OHN)$ allows the determination of the valence bond orders, p_{XH} , by employing empirical correlations. Subsequently, the atomic distances can be derived from the bond orders. To fit the parabolic curve, several ketimine/acid complexes with different acidic and basic properties were analyzed. Strictly ionic species with moderate H-bonds were prepared by using HBF₄ as the acid. Neutral H-

bond complexes were obtained with acetic acid or phenols. (*R*)-TRIP was shown to form strong H-bonds with ion-pair character, as indicated by the strict parabolic progression (Figure 8c). Moreover, the combination of the distances obtained from the Steiner–Limbach correlation and the trans hydrogen scalar coupling analysis revealed that the H-bond is nearly linear and is not influenced by the imine substitution. This analysis proved that the very strong charge-assisted H-bond in the TRIP/imine complexes acts as a structural anchor and may explain the high substrate tolerance of CPA-catalyzed transformations.³²

Parallel to the H-bond study, structural characterization of the binary complex was conducted using NMR spectroscopy and validated by quantum-chemical calculations.³⁴ To achieve the highest sensitivity possible and to determine the buildup linear region, 1D ¹H,¹H selective NOESY buildup studies were used, and they allowed the distance information to be determined (Figure 9). However, the low temperatures

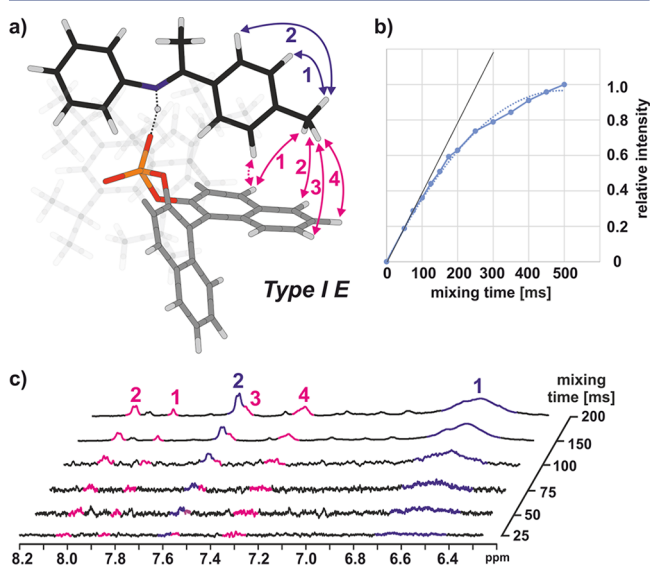


Figure 9. (a) Calculated structure and experimental NOEs of a type I *E* binary complex. (b) NOE buildup curve. (c) Stacked plot showing the 1D selective NOESY spectra at 180 K in CD₂Cl₂ with different τ_{mix} . Adapted from ref 34. Copyright 2016 American Chemical Society.

necessary for the separation of the *E* and *Z* complexes led to large correlation times similar to those required for small proteins, which caused deviations from linearity even with τ_{mix} below 100 ms (Figure 9b). When used in conjunction with the low signal intensities, this allowed for a qualitative interpretation of the NOEs (Figure 9a,c).

Nevertheless, the combination of the known H-bond geometry and the NOE pattern allowed us to determine the core structures of the binary complexes. The possible arrangements of the *E*- and *Z*-imine isomers with respect to the catalyst were calculated, and four core conformations were found (denoted type I/II *E* and type I/II *Z*).^{28b,34}

In general, only one set of imine signals was observed in the complex, but the NOE pattern suggested two core structures. This result indicated that type I/II structures quickly exchange even at 180 K. Our structural analysis showed that the core structures are related by rotation and/or tilting by switching the H-bond acceptor. For the *E*-imine, the desymmetrization of the catalyst backbone clearly showed that type I *E* → type II *E* interconversion occurs via imine tilting inside the complex (imine oxygen switch; Figure 10a). In contrast, for the *Z*-imine, the signals of the two halves of BINOL are completely averaged. In this case, rotation and tilting are allowed because of the compact structure of the *Z*-imine (Figure 11a). Furthermore, the NCI analysis showed that the binary complex is further stabilized by many dispersive interactions. For the *E*-imine, CH– π and π – π interactions between BINOL and the aromatic imine were observed in type I *E* and type II *E* complexes, respectively. For the *Z* complexes, type II *Z* is stabilized by interactions between the aniline ring and the binaphthyl backbone (Figure 11b). The coexistence of the four core structures is seen in each series of aromatic imines investigated regardless of their electronic properties.

Our NMR studies showed that precatalyst complexes can be surprisingly dynamic even at 180 K despite the presence of a strong H-bond. In particular, switching between degenerate H-bond acceptors seems to have a very low activation barrier. In applying these results to catalysis, this analysis proved that the high structural invariance is caused by the strong H-bonds, hinting that dispersive interactions contribute to the high stereoselection observed for CPA catalysts.

Experimental information about prereacting complexes is extremely important for mechanistic understanding. Never-

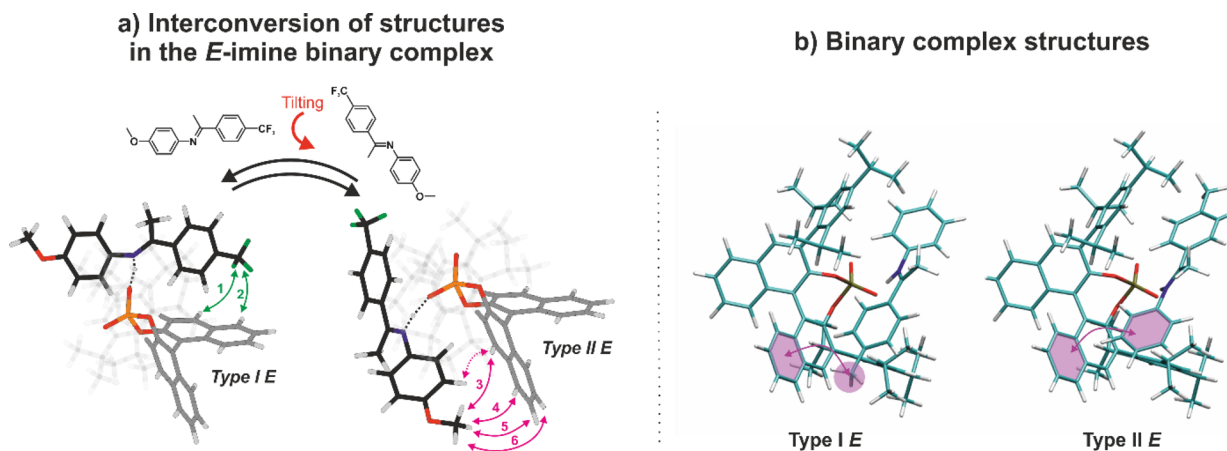


Figure 10. (a) Interconversion of type I/II *E* structures at 180 K by switching the H-bond acceptor. (b) Stabilization of the *E*-imine binary complexes by dispersive interactions. Adapted from ref 34. Copyright 2016 American Chemical Society.

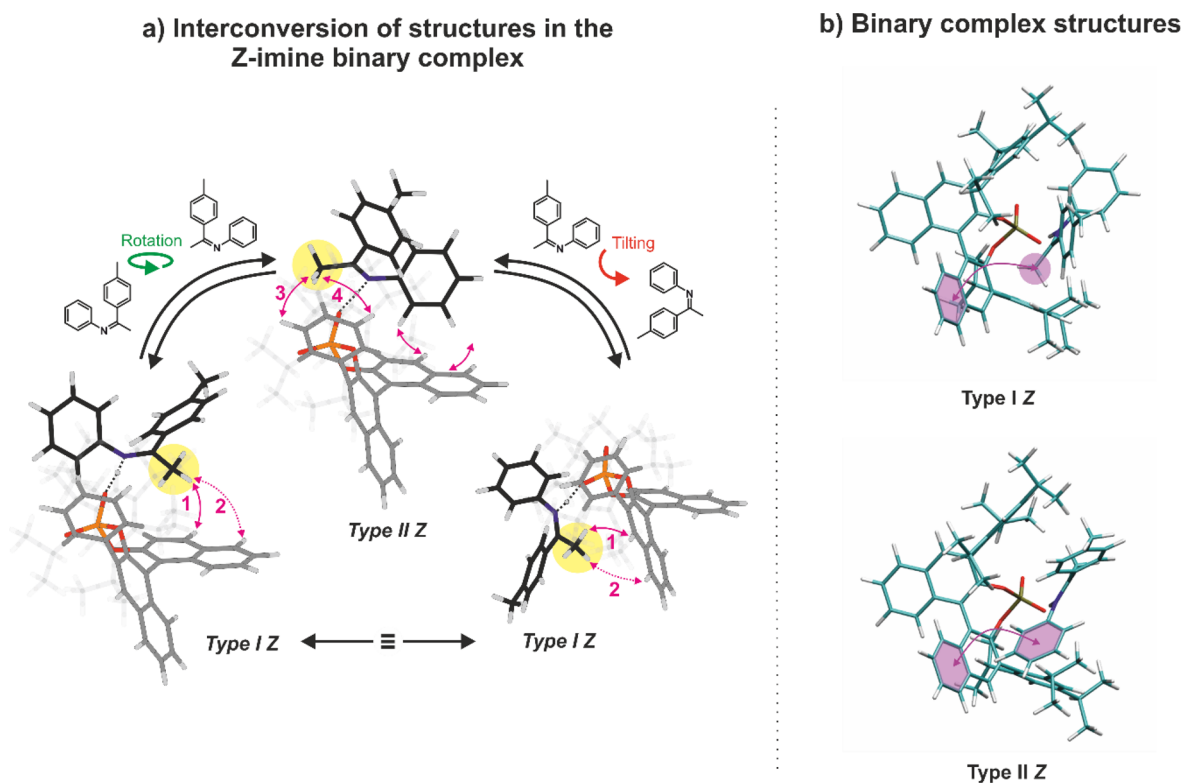


Figure 11. (a) Interconversion of type I/II Z structures via rotation and tilting. (b) Stabilization of Z-imine binary complexes by dispersive interactions. Adapted from ref 34. Copyright 2016 American Chemical Society.

theless, the knowledge of the TSs is vital for comprehending the outcome of a stereo- or regioselective reaction, especially in Curtin–Hammett scenarios and kinetically controlled transformations. To date, direct detection of activated complexes has been possible only for elementary reactions using femtosecond time-resolved spectroscopy.³⁵ Because of poor time resolution, NMR spectroscopy does not allow analysis of the TSs. Therefore, theoretical calculations are generally used. However, we recently developed and applied a general strategy to experimentally elucidate the active TS combinations.³⁶ This technique exploits an external stimulus orthogonal to the reaction mechanism to modulate the equilibrium of slowly exchanging prereacting complexes. As outlined in Figure 12, the modification of the reaction outcome (rate and/or *ee* (ΔP)) is correlated with the change in the populations of intermediates

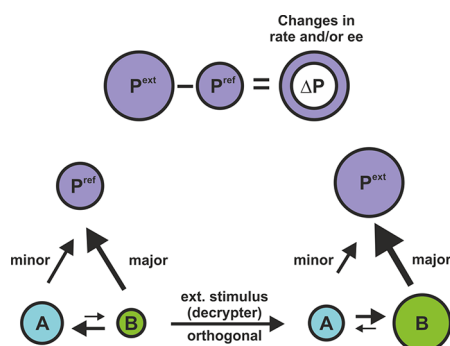


Figure 12. Basic concept of experimental determination of TS combinations. In the DTS- $h\nu$ method, light is used as external stimulus (decrypter) to affect the equilibrium of slowly exchanging intermediates (A and B).³⁶

A and B and reveals the active/major pathway. In this case, the pathway originating from intermediate B is the least demanding (major, Figure 12), and increasing the population of B will accelerate the reaction and/or eventually produce a higher *ee* value (Figure 13, scenario 3). The applied external stimulus works as a mechanistic decrypter. Since in our model reaction light is employed as the external stimulus, the method is called decrypting TS by light (DTS- $h\nu$) (Figure 13). Evaluation of the changes in the characteristic fingerprint pattern (*ee* and reaction rate) upon illumination, as described in Figure 13, allows deep mechanistic insight and reveals for the first time in a purely experimental manner the TSs involved in the reaction under study.

Mechanistic insight into the transfer hydrogenation of the imine was provided by the DFT calculations of Himo and Goodman.²⁸ A three-point interaction model was proposed for the TS, and the Z isomer was postulated to be the reactive species. Generally, the principle described above can be extended to resolve the TS involved in our model reaction. The light used as the external stimulus induces *E* → *Z* isomerization and increases the population of the putative reactive intermediate. When the *E* and *Z* pathways are competing, the rate and *ee* of the reaction should be amplified with increasing content of the Z-imine. However, the mechanism of the real reaction is more complicated. Given two possible sites of nucleophilic attack and two configurational isomers, there are four possible TSs and four possible scenarios leading to the correct enantiomeric product (Figure 13).

Since no change in the enantioselectivity was observed with the increase in reaction rate upon illumination, we proved experimentally that ketimine reduction proceeds exclusively via the Z pathway (Figure 13, scenario 2). The structural and NCI analyses demonstrated that the destabilization of TS-*E* is due to

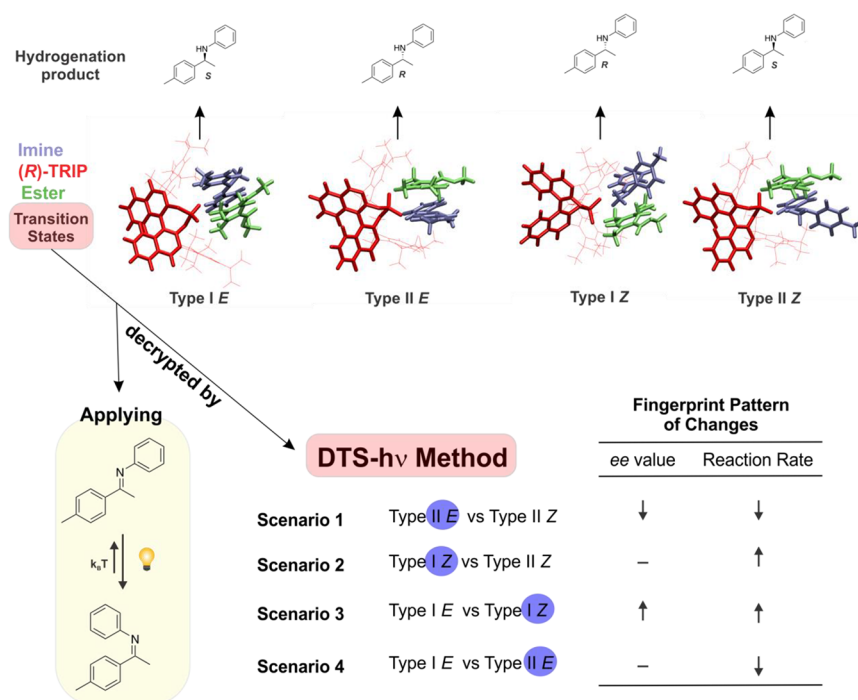


Figure 13. DTS- $h\nu$: illumination causes *E*-imine \rightarrow *Z*-imine interconversion. The effective reaction rate is increased without changing the *ee*, indicating that scenario 2 is active. Adapted from ref 36. Copyright 2016 American Chemical Society.

the extended structure of the *E*-imine, which causes elongation and weakening of the H-bond between the imine and CPA. In contrast, the more compact structure of the *Z*-imine allows the formation of a stronger H-bond in the TS.

Both our NMR investigation and the results of the DTS- $h\nu$ method showed that the imine isomerization is slow. Overall, DTS- $h\nu$ provides the first purely experimental access to the TS combinations by illuminating the reaction and comparing the obtained reaction rate and enantioselectivity to those obtained from reactions conducted in the dark. The method can be applied when there is no significant photodegradation and the principal reaction mechanism does not change upon irradiation.

CONCLUSIONS

This Account has summarized the work done in our research group in the past 7 years on the detection and characterization of elusive intermediates in organocatalysis and experimental access to TS combinations. Detailed mechanistic investigations were made possible by combining NMR spectroscopy, adaptation of synthetic procedures to NMR requirements, theoretical calculations, and photoisomerization. We have established a synergy between different strategies that may benefit other research fields by direct transfer of the general concepts we have developed.

AUTHOR INFORMATION

Corresponding Author

*E-mail: ruth.gschwind@chemie.uni-regensburg.de.

ORCID

Polyssena Renzi: 0000-0002-1326-8183

Ruth M. Gschwind: 0000-0003-3052-0077

Author Contributions

The manuscript was written through contributions of all authors. All authors have given approval to the final version of the manuscript.

Funding

European Research Council (ERC-CoG 614182 – IonPairsAt-Catalysis) and the German Science Foundation (DFG-GRK 1626, Chemical Photocatalysis; DFG-GS 13/4-1).

Notes

The authors declare no competing financial interest.

Biographies

Polyssena Renzi was born in Rome, Italy, in 1987. She completed her Ph.D. in 2014 at Sapienza University of Rome under the supervision of Professor M. Bella, working on the development of new strategies for asymmetric reactions. In 2015 she joined the group of Professor R. M. Gschwind at Regensburg University (Germany) as a postdoctoral researcher, where she is currently investigating the mechanisms of organocatalyzed reactions using NMR methods.

Johnny Hioe was born in Jakarta, Indonesia, in 1983. He completed his dissertation at Ludwig Maximilian University of Munich under the supervision of Prof. H. Zipse, working on the thermodynamic stability of radicals in biological systems. In 2014 he joined the group of Prof. R. M. Gschwind at Regensburg University (Germany) as a postdoctoral researcher, where he is currently investigating the mechanism of organocatalyzed reactions using theoretical calculations.

Ruth M. Gschwind obtained her Ph.D. from TU Munich in 1997 and finished her habilitation in 2002 at the University of Marburg. From 2002 to 2005, she was a professor at the University of Bonn. In 2005 she joined the University of Regensburg as a professor of organic chemistry. Her research focuses are the stabilization and characterization of catalyst complexes, reaction intermediates, and H-bonds as well as the elucidation of reaction mechanisms of organo-, photo-, and transition-metal-catalyzed reactions by NMR spectroscopy.

■ REFERENCES

- (1) (a) Melchiorre, P.; Marigo, M.; Carlone, A.; Bartoli, G. Asymmetric Aminocatalysis—Gold Rush in Organic Chemistry. *Angew. Chem., Int. Ed.* **2008**, *47*, 6138–6171. (b) Bertelsen, S.; Jørgensen, K. A. Organocatalysis after the gold rush. *Chem. Soc. Rev.* **2009**, *38*, 2178–2189.
- (2) (a) Pihko, P. M.; Majander, I.; Erkkilä, A. Enamine Catalysis. *Top. Curr. Chem.* **2010**, *291*, 29–75. (b) Mukherjee, S.; Yang, J. W.; Hoffmann, S.; List, B. Asymmetric Enamine Catalysis. *Chem. Rev.* **2007**, *107*, 5471–5569.
- (3) Hajos, Z. G.; Parrish, D. R. Asymmetric synthesis of bicyclic intermediates of natural product chemistry. *J. Org. Chem.* **1974**, *39*, 1615–1621.
- (4) Schmid, M. B.; Zeitler, K.; Gschwind, R. M. The Elusive Enamine Intermediate in Proline-Catalyzed Aldol Reactions: NMR Detection, Formation Pathway, and Stabilization Trends. *Angew. Chem., Int. Ed.* **2010**, *49*, 4997–5003.
- (5) Bock, D. A.; Lehmann, C. W.; List, B. Crystal structures of proline-derived enamines. *Proc. Natl. Acad. Sci. U. S. A.* **2010**, *107*, 20636–20641.
- (6) Seebach, D.; Boes, M.; Naef, R.; Schweizer, W. B. Alkylation of Amino Acids without Loss of the Optical Activity: Preparation of α -Substituted Proline Derivatives. A Case of Self-Reproduction of Chirality. *J. Am. Chem. Soc.* **1983**, *105*, 5390–5398.
- (7) Schmid, M. B.; Zeitler, K.; Gschwind, R. M. Formation and Stability of Prolinol and Prolinol Ether Enamines by NMR: Delicate Selectivity and Reactivity Balances and Parasitic Equilibria. *J. Am. Chem. Soc.* **2011**, *133*, 7065–7074.
- (8) Haindl, M. H.; Hioe, J.; Gschwind, R. M. The Proline Enamine Formation Pathway Revisited in Dimethyl Sulfoxide: Rate Constants Determined via NMR. *J. Am. Chem. Soc.* **2015**, *137*, 12835–12842.
- (9) List, B.; Lerner, R. A.; Barbas, C. F. Proline-Catalyzed Direct Asymmetric Aldol Reactions. *J. Am. Chem. Soc.* **2000**, *122*, 2395–2396.
- (10) Bahmanyar, S.; Houk, K. N.; Martin, H. J.; List, B. Quantum Mechanical Predictions of the Stereoselectivities of Proline-Catalyzed Asymmetric Intermolecular Aldol Reactions. *J. Am. Chem. Soc.* **2003**, *125*, 2475–2479.
- (11) Sharma, A. K.; Sunoj, R. B. Enamine versus Oxazolidinone: What Controls Stereoselectivity in Proline-Catalyzed Asymmetric Aldol Reactions? *Angew. Chem., Int. Ed.* **2010**, *49*, 6373–6377.
- (12) Seebach, D.; Beck, A. K.; Badine, M.; Limbach, M.; Eschenmoser, A.; Treasurywala, A. M.; Hobi, R.; Prikoszovich, W.; Linder, B. Are Oxazolidinones Really Unproductive, Parasitic Species in Proline Catalysis?—Thoughts and Experiments Pointing to an Alternative View. *Helv. Chim. Acta* **2007**, *90*, 425–471.
- (13) (a) Riplinger, C.; Sandhoefer, B.; Hansen, A.; Neese, F. Natural triple excitations in local coupled cluster calculations with pair natural orbitals. *J. Chem. Phys.* **2013**, *139*, 134101–134113. (b) Riplinger, C.; Neese, F. An efficient and near linear scaling pair natural orbital based local coupled cluster method. *J. Chem. Phys.* **2013**, *138*, 034106–034118.
- (14) (a) Hein, J. E.; Burés, J.; Lam, Y.-h.; Hughes, M.; Houk, K. N.; Armstrong, A.; Blackmond, D. G. Enamine Carboxylates as Stereo-determining Intermediates in Prolinate Catalysis. *Org. Lett.* **2011**, *13*, 5644–5647. (b) Patil, M. P.; Sunoj, R. B. Insights on Co-Catalyst-Promoted Enamine Formation between Dimethylamine and Propanal through Ab Initio and Density Functional Theory Study. *J. Org. Chem.* **2007**, *72*, 8202–8215. (c) Hall, N. E.; Smith, B. J. High-Level ab Initio Molecular Orbital Calculations of Imine Formation. *J. Phys. Chem. A* **1998**, *102*, 4930–4938.
- (15) Ashley, M. A.; Hirschi, J. S.; Izzo, J. A.; Veticatt, M. J. Isotope Effects Reveal the Mechanism of Enamine Formation in *l*-Proline-Catalyzed α -Amination of Aldehydes. *J. Am. Chem. Soc.* **2016**, *138*, 1756–1759.
- (16) Schmid, M. B.; Zeitler, K.; Gschwind, R. M. Distinct conformational preferences of prolinol and prolinol ether enamines in solution revealed by NMR. *Chem. Sci.* **2011**, *2*, 1793–1803.
- (17) Allemann, C.; Um, J. M.; Houk, K. N. Computational investigations of the stereoselectivities of proline-related catalysts for aldol reactions. *J. Mol. Catal. A: Chem.* **2010**, *324*, 31–38.
- (18) Seegerer, A.; Hioe, J.; Hammer, M. M.; Morana, F.; Fuchs, P. J. W.; Gschwind, R. M. Remote-Stereocontrol in Dienamine Catalysis: *Z*-Dienamine Preferences and Electrophile–Catalyst Interaction Revealed by NMR and Computational Studies. *J. Am. Chem. Soc.* **2016**, *138*, 9864–9873.
- (19) Seebach, D.; Gilmour, R.; Grošelj, U.; Deniau, G.; Sparr, C.; Ebert, M.-O.; Beck, A. K.; McCusker, L. B.; Šišak, D.; Uchamaru, T. Stereochemical Models for Discussing Additions to α,β -Unsaturated Aldehydes Organocatalyzed by Diarylprolinol or Imidazolidinone Derivatives—Is There an '(E)/(Z)-Dilemma'? *Helv. Chim. Acta* **2010**, *93*, 603.
- (20) Bertelsen, S.; Marigo, M.; Brandes, S.; Dinér, P.; Jørgensen, K. A. Dienamine Catalysis: Organocatalytic Asymmetric γ -Amination of α,β -Unsaturated Aldehydes. *J. Am. Chem. Soc.* **2006**, *128*, 12973–12980.
- (21) Johnson, E. R.; Keinan, S.; Mori-Sánchez, P.; Contreras-García, J.; Cohen, A. J.; Yang, W. Revealing Noncovalent Interaction. *J. Am. Chem. Soc.* **2010**, *132*, 6498–6506.
- (22) Rueping, M.; Parmar, D.; Sugiono, E. *Asymmetric Brønsted Acid Catalysis*; Wiley-VCH: Weinheim, Germany, 2016.
- (23) Mahlau, M.; List, B. Asymmetric Counteranion-Directed Catalysis: Concept, Definition, and Applications. *Angew. Chem., Int. Ed.* **2013**, *52*, 518–533.
- (24) Grzesiek, S.; Cordier, F.; Jaravine, V.; Barfield, M. Insights into biomolecular hydrogen bonds from hydrogen bond scalar couplings. *Prog. Nucl. Magn. Reson. Spectrosc.* **2004**, *45*, 275–300.
- (25) Limbach, H.-H.; Chan-Huot, M.; Sharif, S.; Tolstoy, P. M.; Shenderovich, I. G.; Denisov, G. S.; Toney, M. D. Crytical hydrogen bonds and protonation states of pyridoxal 5'-phosphate revealed by NMR. *Biochim. Biophys. Acta, Proteins Proteomics* **2011**, *1814*, 1426–1437.
- (26) (a) Gschwind, R. M.; Armbrüster, M.; Zubrzycki, I. Z. NMR Detection of Intermolecular NH–OP Hydrogen Bonds between Guanidinium Protons and Bisphosphonate Moieties in an Artificial Arginine Receptor. *J. Am. Chem. Soc.* **2004**, *126*, 10228–10229. (b) Federwisch, G.; Kleinmaier, R.; Drettwan, D.; Gschwind, R. M. The H-Bonding Network of Acylguanidine Complexes: Combined Intermolecular $^2\text{J}_{\text{H,P}}$ and $^3\text{J}_{\text{H,P}}$ Scalar Couplings Provide an Insight into the Geometric Arrangement. *J. Am. Chem. Soc.* **2008**, *130*, 16846–16847.
- (27) (a) Hoffmann, S.; Seayad, A. M.; List, B. A Powerful Brønsted Acid Catalyst for the Organocatalytic Asymmetric Transfer Hydrogenation of Imines. *Angew. Chem., Int. Ed.* **2005**, *44*, 7424–7427. (b) Rueping, M.; Sugiono, E.; Azap, C.; Theissmann, T.; Bolte, M. Enantioselective Brønsted Acid Catalyzed Transfer Hydrogenation: Organocatalytic Reduction of Imines. *Org. Lett.* **2005**, *7*, 3781–3783.
- (28) (a) Marcelli, T.; Hammar, P.; Himo, F. Phosphoric Acid Catalyzed Enantioselective Transfer Hydrogenation of Imines: A Density Functional Theory Study of Reaction Mechanism and the Origins of Enantioselectivity. *Chem. - Eur. J.* **2008**, *14*, 8562–8571. (b) Simón, L.; Goodman, J. M. Theoretical Study of the Mechanism of Hantzsch Ester Hydrogenation of Imines Catalyzed by Chiral BINOL-Phosphoric Acids. *J. Am. Chem. Soc.* **2008**, *130*, 8741–8747.
- (29) Tang, W.; Johnston, S.; Iggo, J. A.; Berry, N. G.; Phelan, M.; Lian, L.; Bacsa, J.; Xiao, J. Cooperative Catalysis through Noncovalent Interactions. *Angew. Chem., Int. Ed.* **2013**, *52*, 1668–1672.
- (30) (a) Storer, R. I.; Carrera, D. E.; Ni, Y.; MacMillan, D. W. C. Enantioselective Organocatalytic Reductive Amination. *J. Am. Chem. Soc.* **2006**, *128*, 84–86. (b) Sickert, M.; Abels, F.; Lang, M.; Sieler, J.; Birkemeyer, C.; Schneider, C. *Chem. - Eur. J.* **2010**, *16*, 2806–2818.
- (31) Fleischmann, M.; Drettwan, D.; Sugiono, E.; Rueping, M.; Gschwind, R. M. Brønsted Acid Catalysis: Hydrogen Bonding versus Ion Pairing in Imine Activation. *Angew. Chem., Int. Ed.* **2011**, *50*, 6364–6369.
- (32) Sorgenfrei, N.; Hioe, J.; Greindl, J.; Rothermel, K.; Morana, F.; Lokesh, N.; Gschwind, R. M. NMR Spectroscopic Characterization of

Charge Assisted Strong Hydrogen Bonds in Brønsted Acid Catalysis. *J. Am. Chem. Soc.* **2016**, *138*, 16345–16354.

(33) (a) Benedict, H.; Shenderovich, I. G.; Malkina, O. L.; Malkin, V. G.; Denisov, G. S.; Golubev, N. S.; Limbach, H.-H. Nuclear Scalar Spin-Spin Couplings and Geometries of Hydrogen Bonds. *J. Am. Chem. Soc.* **2000**, *122*, 1979–1988. (b) Limbach, H.-H.; Pietrzak, M.; Sharif, S.; Tolstoy, P. M.; Shenderovich, I. G.; Smirnov, S. N.; Golubev, N. S.; Denisov, G. S. NMR Parameters and Geometries of OHN and ODN Hydrogen Bonds of Pyridine–Acid Complexes. *Chem. - Eur. J.* **2004**, *10*, 5195–5204. (c) Sharif, S.; Denisov, G. S.; Toney, M. D.; Limbach, H.-H. NMR Studies of Coupled Low- and High-Barrier Hydrogen Bonds in Pyridoxal-5'-phosphate Model Systems in Polar Solution. *J. Am. Chem. Soc.* **2007**, *129*, 6313–6327.

(34) Greindl, J.; Hioe, J.; Sorgenfrei, N.; Morana, F.; Gschwind, R. M. Brønsted Acid Catalysis-Structural Preferences and Mobility in Imine/Phosphoric Acid Complexes. *J. Am. Chem. Soc.* **2016**, *138*, 15965–15971.

(35) Dietze, D. R.; Mathies, R. A. Femtosecond Stimulated Raman Spectroscopy. *ChemPhysChem* **2016**, *17*, 1224–1251.

(36) Renzi, P.; Hioe, J.; Gschwind, R. M. Decrypting Transition States by Light: Photoisomerization as a Mechanistic Tool in Brønsted Acid Catalysis. *J. Am. Chem. Soc.* **2017**, *139*, 6752–6760.